

# Natural Abundance $^{17}\text{O}$ DNP NMR Provides Precise O-H Distances and Insights into the Brønsted Acidity of Heterogeneous Catalysts

Frédéric A. Perras, Zhuoran Wang, Pranjali Naik, Igor I. Slowing, and Marek Pruski\*

**Abstract:** Heterogeneous Brønsted acid catalysts are tremendously important in industry, particularly in catalytic cracking processes. Here we show that these Brønsted acid sites can be directly observed at natural abundance by  $^{17}\text{O}$  DNP surface-enhanced NMR spectroscopy (SENS). We additionally show that the O–H bond length in these catalysts can be measured with a sub-pm precision, to enable a direct structural gauge of the lability of protons in a given material, which is correlated with the material's pH of zero point of charge. Experiments performed on materials impregnated with pyridine also allow for the direct detection of intermolecular hydrogen bonding interactions through the lengthening of O–H bonds.

Brønsted acid sites, found at the surfaces of oxide materials, are of utmost importance in a number of industrial processes, most notably fluid catalytic cracking of petroleum hydrocarbons. Crystalline zeolites have historically been the predominant solid acid catalyst used in the petrochemical industry; however, these are plagued with coking, which blocks the pores and necessitates frequent regeneration.<sup>[1]</sup> Remedies to catalyst deactivation include the use of solid Brønsted acid catalysts possessing larger pores, such as mesoporous silica and, most notably, silica-alumina.<sup>[2]</sup> Contrary to zeolites, however, these materials are generally amorphous, which significantly impacts our ability to characterize them at the atomic level.

Solid-state nuclear magnetic resonance (SSNMR) spectroscopy is arguably the most diagnostic technique for atomic-scale characterization of catalytically important sites in amorphous heterogeneous catalysts.<sup>[3]</sup> However, the Brønsted acid sites are recognized as surface hydroxyls, which challenges their characterization by conventional SSNMR. Although a large body of work has been compiled using  $^1\text{H}$  SSNMR to characterize these hydroxyls, generally only qualitative information about Brønsted acidity can be gained from such studies. It was notably shown that the  $^1\text{H}$  chemical shift is correlated with the vibrational stretching frequency as well as the electronegativity of the material.<sup>[4]</sup> The only NMR-active isotope of oxygen,  $^{17}\text{O}$ , is quadrupolar ( $I = 5/2$ ) and has an extremely low natural abundance of 0.038%. With the use of  $^{17}\text{O}$  SSNMR being constrained by the need of isotope enrichment, which is both expensive and synthetically challenging, very few studies utilized the  $^{17}\text{O}$  nuclide. Notable exceptions include zeolites, and other oxides, which can be easily enriched with  $\text{O}_2$  gas at high temperatures.<sup>[5,6]</sup> Recently, however, a number of reports have shown that  $^{17}\text{O}$  SSNMR can indeed be performed at natural abundance using dynamic nuclear polarization (DNP).<sup>[7]</sup> DNP enhances the signal of nuclear spins by a microwave-induced polarization transfer from exogenously introduced unpaired

electrons.<sup>[8]</sup> Theoretically, DNP can exceed the Boltzmann polarization of  $^{17}\text{O}$  nuclei by a factor of 4855.<sup>[9]</sup> Since DNP can also easily enhance the signals from surfaces—a technique called DNP surface-enhanced NMR spectroscopy (SENS)<sup>[10]</sup>—it enables a transformative expansion of applications of  $^{17}\text{O}$  SSNMR spectroscopy. Here, we demonstrate that natural-abundance  $^{17}\text{O}$  DNP SENS can directly probe the Brønsted acidity of surface hydroxyls in silica and silica-alumina materials. Most notably, it allowed us to determine the O–H bond lengths in these materials with an unprecedented, sub-pm precision.

Hydroxyl moieties in silica and alumina materials can be found in a number of different coordination modes. For silica, all hydroxyls are present as silanols ( $\text{SiOH}$ ) while on alumina, both non-bridging and bridging aluminols ( $\text{Al}_n\text{OH}$ ,  $n=1, 2,$  and  $3$ ) are possible.<sup>[11]</sup> In silica-alumina, all four types can be present, along with an additional bridging type ( $\text{Al}(\text{OH})\text{Si}$ ), which is typically credited for the material's Brønsted acidity.<sup>[3]</sup> Unfortunately, the large quadrupolar coupling of these sites hinders their resolution by  $^{17}\text{O}$  SSNMR. Luckily, however, they do possess a reasonable dispersion of chemical shifts with minimal interference from second-order quadrupole shifts since the distribution of  $C_Q$  is far greater than the differences between sites.<sup>[12]</sup> The  $^{17}\text{O}$  lineshape is therefore expected to be sensitive to the different hydroxyl environments present in a sample. For example, at 9.4 T,  $\mu_1$ -aluminols are expected to have a center of mass of -13 ppm while  $\mu_2$ -aluminols would resonate at -35 ppm,<sup>[13]</sup> silanols would resonate at -65 ppm,<sup>[7 b,c],[14]</sup> and  $\text{Al}(\text{OH})\text{Si}$  sites at -48 ppm.<sup>[5,12]</sup>

The  $^{17}\text{O}\{^1\text{H}\}$ , DNP-enhanced SSNMR spectrum of an MCM-41-type mesoporous silica nanoparticle (MSN) sample that was acquired using the PRESTO-QCPMG technique<sup>[7b]</sup> (phase-shifted recoupling effects a smooth transfer of polarization<sup>[15]</sup> quadrupolar Car-Purcell-Meiboom-Gill<sup>[16]</sup>), shown in Figure 1, presents a broad resonance centered at -65 ppm, as expected. The spectrum acquired on 5% silica-alumina was markedly different, however, featuring a dominant peak at -15 ppm as well as a smaller shoulder at  $\sim$ -40 ppm, which could be assigned to the  $\mu_1$ - and  $\mu_2$ -aluminols, respectively. Since this material is essentially boehmite, the dominance of  $\mu_1$ -aluminols is expected. Upon calcination, which serves to activate the catalyst, the majority of the  $\mu_1$ -aluminols are removed, leaving the more acidic bridging hydroxyls.<sup>[17]</sup> The  $^{17}\text{O}$  spectrum of 40% silica-alumina is the broadest due to the overlap of the signals from silanols (-65 ppm) and aluminols (-13 and -35 ppm). In this case, calcination noticeably narrows the spectrum since the silanols and non-bridging aluminols are dehydroxylated, leaving the bridging aluminols and  $\text{Al}(\text{OH})\text{Si}$  sites, which possess similar resonance frequencies. Interestingly also, if this sample is impregnated with pyridine, the center of mass of the resonance relocates to a higher chemical shift. This can be explained by the fact that the  $\text{Al}(\text{OH})\text{Si}$  sites have a high Brønsted acidity and are deprotonated by pyridine,<sup>[18]</sup> thus eliminating their  $^{17}\text{O}\{^1\text{H}\}$  PRESTO signal.

[\*] Dr. F. A. Perras, Z. Wang, P. Naik, Prof. I.I. Slowing, Prof. M. Pruski  
U.S. DOE Ames Laboratory, and Department of Chemistry, Iowa  
State University  
Ames, IA 50011, USA  
E-mail: mpruski@iastate.edu

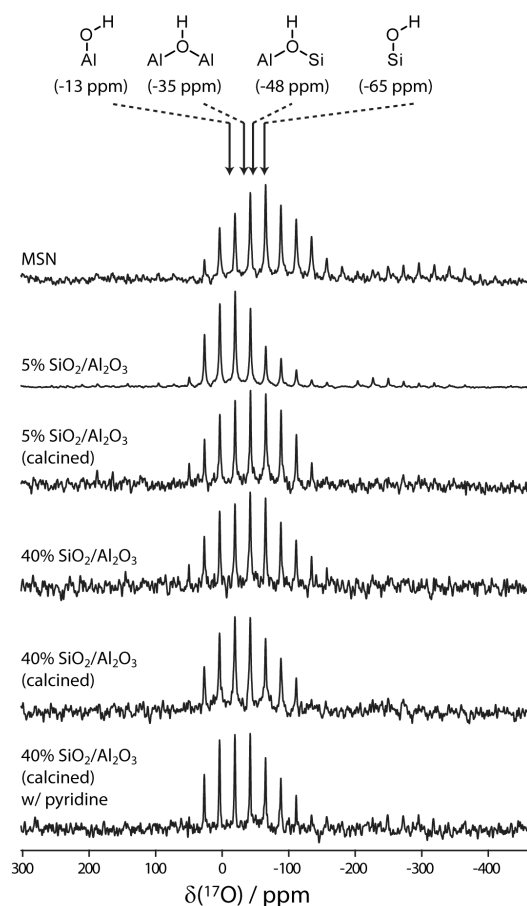


**Figure 1.** DNP-enhanced, natural-abundance,  $^{17}\text{O}\{^1\text{H}\}$  PRESTO-QCPMG spectra acquired on various silica and silica-alumina samples, as indicated in the Figure. The expected centers of mass for four different hydroxyl environments are indicated at the top. Note that the positions of individual QCPMG spikelets are determined by the  $^{17}\text{O}$  transmitter frequency, which was set to the same value in all spectra.

In order to probe the acidity of the Brønsted acid sites more directly, we sought to measure the O–H bond lengths in these systems since it is expected to be related to the acidity of the proton—longer O–H distances being characteristic of a more labile, and thus more acidic, proton.<sup>[5]</sup> In previous studies, we used PRESTO dipolar oscillations to probe  $^{17}\text{O}$ – $^1\text{H}$  dipolar coupling and distinguish signals originating from rigid and mobile silanols.<sup>[7b,c]</sup> Although this approach can easily distinguish dynamic and static hydroxyls, since their averaged dipolar coupling constants ( $R_{\text{DD}}$ ) differ by roughly 50%, this approach is easily perturbed by the rf field inhomogeneity and mismatch, as well as the  $^1\text{H}$  chemical shift anisotropy (CSA).<sup>[15]</sup> A more robust technique is required to measure precise differences in O–H bond lengths.

For this purpose we chose to apply the windowed-proton-detected local-field (wPDLF) technique.<sup>[19]</sup> The use of a windowed  $R$  element dramatically increases the robustness of the sequence with respect to RF mismatch<sup>[19b],[20]</sup> and also increases the scaling factor of the recoupled dipolar coupling.<sup>[21]</sup> wPDLF also includes a phase shift of the recoupling block which serves to refocus the  $^1\text{H}$  CSA while an  $^{17}\text{O}$  inversion pulse

prevents the same refocusing from occurring for the  $^{17}\text{O}$ – $^1\text{H}$  dipolar coupling. The technique can also be combined with PRESTO-QCPMG and thus enable detection at natural abundance. Lastly, since the dipolar oscillations can be Fourier transformed to yield a simple doublet, no curve fitting is necessary and the dipolar coupling can be determined to high accuracy by measuring the splitting of the doublet.

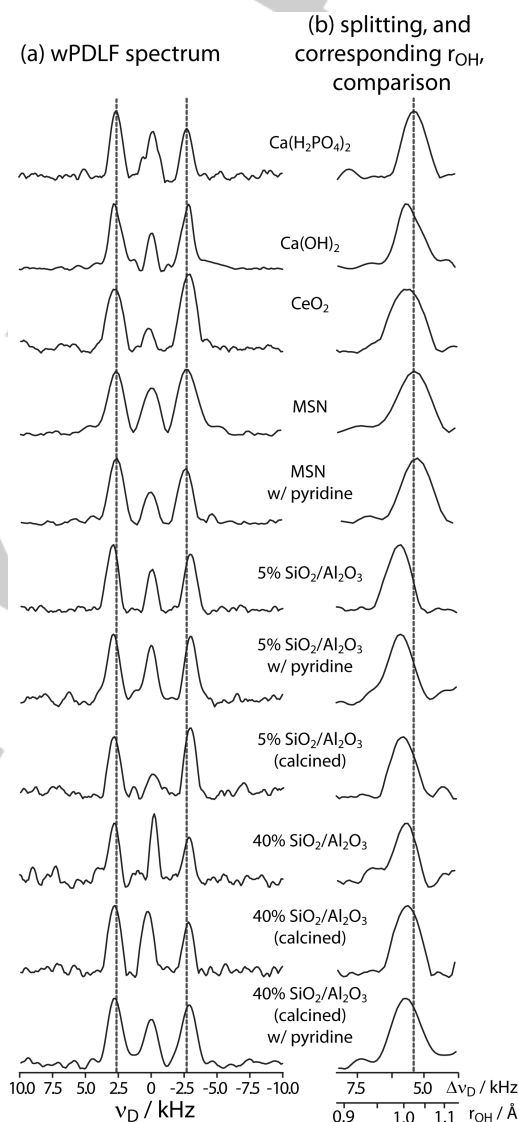


**Figure 2.** DNP-enhanced, natural-abundance  $^{17}\text{O}\{^1\text{H}\}$  wPDLF-QCPMG spectra are shown in (a) for all materials discussed in the text, as indicated on the Figure. Dashed lines are added to highlight the splitting observed in  $\text{Ca}(\text{H}_2\text{PO}_4)_2$  and to aid in the comparison of spectra. Enlarged views of the higher-frequency peak are shown in (b). In order to highlight the differences in the splittings, the position of the low-frequency peak was fixed to 0 kHz.

wPDLF-QCPMG spectra measured on the same samples as in Figure 1 are shown in Figure 2 with the results presented in Table 1. Along with those samples, the O–H bond lengths in ceria nanoparticles,<sup>[22]</sup>  $\text{Ca}(\text{OH})_2$ , a base, and  $\text{Ca}(\text{H}_2\text{PO}_4)_2$ , which possesses acidic protons, were also measured. Very sharp and

well-defined doublets were obtained indicating that dynamic averaging is largely negligible, with the possible exception of silica. Note that the use of low temperatures is known to freeze O–H dynamics and lead to more accurate distance measurements<sup>[5c]</sup> and that the use of a PRESTO polarization transfer emphasizes the most rigid hydroxyls. Remarkably, we found that the O–H distance measured by <sup>17</sup>O wPDLF is inversely correlated with the pH of the zero point of charge (pH<sub>ZPC</sub>, see Figure 3), a common measure of the acidity of oxide surfaces,<sup>[23]</sup> thus confirming the hypothesis that a proton's lability is correlated with the O–H bond length.

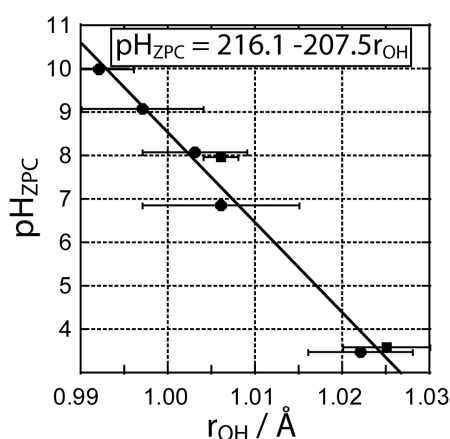


**Figure 3.** The O–H distances measured by <sup>17</sup>O wPDLF are plotted against the pH<sub>ZPC</sub> values of the various materials taken from the literature.<sup>[23]</sup> The square data points correspond to Ca(OH)<sub>2</sub> and Ca(H<sub>2</sub>PO<sub>4</sub>), for which pH<sub>ZPC</sub> values cannot be obtained; equivalent equilibrium constants were instead estimated using their acid-base constants.

**Table 1.** Results from the <sup>17</sup>O{<sup>1</sup>H} wPDLF-QCPMG measurements.

Material	R <sub>BD</sub> / kHz <sup>[a]</sup>	r <sub>OH</sub> <sup>[b]</sup> / Å <sup>[a]</sup>	Δr <sub>OH</sub> <sup>[c]</sup> / pm
Ca(H <sub>2</sub> PO <sub>4</sub> ) <sub>2</sub>	15.1 ± 0.2	1.025 ± 0.005	0.0
Ca(OH) <sub>2</sub>	16.0 ± 0.1	1.006 ± 0.002	-1.8
CeO <sub>2</sub>	16.1 ± 0.3	1.003 ± 0.006	-2.1
MSN	15.3 ± 0.3	1.022 ± 0.006	-0.3
MSN w/ pyridine	14.6 ± 0.2	1.038 ± 0.004	1.4
5% SiO <sub>2</sub> /Al <sub>2</sub> O <sub>3</sub>	16.7 ± 0.2	0.992 ± 0.004	-3.2
5% SiO <sub>2</sub> /Al <sub>2</sub> O <sub>3</sub> w/ pyridine	16.7 ± 0.3	0.992 ± 0.006	-2.3
5% SiO <sub>2</sub> /Al <sub>2</sub> O <sub>3</sub> (calcined)	16.4 ± 0.3	0.997 ± 0.007	-2.7
40% SiO <sub>2</sub> /Al <sub>2</sub> O <sub>3</sub>	16.0 ± 0.4	1.006 ± 0.009	-1.8
40% SiO <sub>2</sub> /Al <sub>2</sub> O <sub>3</sub> (calcined)	15.8 ± 0.4	1.009 ± 0.009	-1.5
40% SiO <sub>2</sub> /Al <sub>2</sub> O <sub>3</sub> (calcined) w/ pyridine	15.8 ± 0.3	1.009 ± 0.006	-1.5

[a] The uncertainties in the splittings were determined as FWHM/(S/N).<sup>[24]</sup> [b] Note that NMR-measured distances correspond to the cubic root of the motional average of the cubed distance. This distance differs from those measured by diffraction and is typically ~3 pm longer.<sup>[25]</sup> The differences between NMR-measured distances is, however, highly accurate.<sup>[26]</sup> [c] This corresponds to the difference in bond length when compared to Ca(H<sub>2</sub>PO<sub>4</sub>)<sub>2</sub>.

As expected, we observed that the O–H bond length is 1.8 pm longer in the case of Ca(H<sub>2</sub>PO<sub>4</sub>)<sub>2</sub> (1.025 Å) than for Ca(OH)<sub>2</sub> (1.006 Å) due to that proton's greater lability. Similarly, we observed a long average O–H bond length in the case of MSN since silanols are known for being Brønsted acidic.<sup>[27]</sup> The

components of the doublet are, however, much broader in this case due to the distribution of O–H bond lengths and the mobility of the silanols.<sup>[7c]</sup> If the MSN sample is impregnated with pyridine-d<sub>5</sub> in a 1:1 pyridine:silanol ratio we observe a further lengthening of the O–H bond by 1.7 pm to 1.038 Å pointing to the formation of intermolecular hydrogen bonds with pyridine.<sup>[28]</sup> Notably, also, the components of the doublet are now sharper, indicating that the O–H bond length is better defined in the presence of this dominant intermolecular interaction.

In the case of 5% silica-alumina, we see that the aluminols have much shorter O–H bond lengths of 0.992 Å (1.4 pm shorter than Ca(OH)<sub>2</sub>). This is in agreement with experimental<sup>[27]</sup> and theoretical<sup>[29]</sup> data showing that silanols are in fact Brønsted acidic while aluminols are Lewis basic. The O–H bond length is unaffected by the addition of pyridine, indicating that the aluminols typically accept intra-surface hydrogen bonds, rather than donate intermolecular ones, in agreement with previous DFT results.<sup>[29]</sup> Calcining the material leads to a slight lengthening of the average O–H bond length, indicating that the bridging aluminols are slightly more acidic than the non-bridging ones. Note that we were unable to resolve the distances for each site and thus the numbers reported in Table 1 represent averages for each surface. These bridging aluminols have 2.4 pm shorter O–H bond lengths than silanols, which is in agreement with the DFT-predicted range of 0.7 to 2.5 pm.<sup>[29]</sup>

For 40% silica-alumina, we measured an O–H bond length that was indistinguishable from that of Ca(OH)<sub>2</sub> and fell in between what was measured for 5% silica-alumina and the MSN. Again, calcination leads to a slight increase in the O–H bond length. This material is also insensitive to the introduction of pyridine, which stems from the fact that the Brønsted acid sites (Si(OH)Al) are rare and deprotonated in the presence of pyridine, *vide supra*. The fact that the average acidity of this material is also intermediate between alumina and silica is in agreement with previous acidity measurements.<sup>[27a] [23b]</sup>

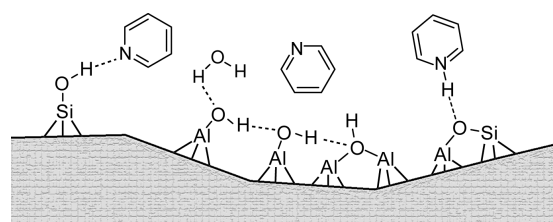


**Figure 4.** A depiction of the silica/alumina surface in the presence of pyridine is shown. Silanols form strong hydrogen bonds with pyridine while the Brønsted acid sites are deprotonated. Aluminols, being far more Lewis basic, do not interact with pyridine and instead form intra-surface hydrogen bonds to other surface sites as well as adsorbed water.

In conclusion, we used natural-abundance <sup>17</sup>O DNP SENS to probe the Brønsted acidity of surface hydroxyls in silica and silica-alumina materials. We have observed that silanols are Brønsted acidic and form strong intermolecular hydrogen bonds with pyridine that lead to an observable lengthening of the O–H bond length (Figure 4). Aluminols, on the other hand, are Lewis basic and are not hydrogen bond donors (Figure 4); we do,

however, see that bridging aluminols are slightly more acidic. In contrast to those of silica, the Brønsted acid sites of silica-alumina are completely deprotonated by pyridine, and are thus very acidic (Figure 4), but the average hydroxyl in this material has an acidity that is between those of pure silica and alumina.

## Experimental Section

Commercial 5% (SIRAL 5) and 40% (SIRAL 40 HPV) silica-alumina samples were obtained from Sasol while the MCM-41-type MSN and ceria samples were prepared as described elsewhere.<sup>[7c][22]</sup> All DNP SSNMR experiments were performed using a Bruker AVANCE III DNP NMR spectrometer equipped with a 263 GHz gyrotron and a 3.2 mm low-temperature magic-angle-spinning (MAS) probe at a temperature of 105 K. For the DNP measurements, the samples were impregnated with 15 to 30 mM TEKPo<sup>[30]</sup> solutions and spun at 12.5 kHz. PRESTO polarization transfer was achieved using a total of 160  $\mu$ s of R18,<sup>7</sup> recoupling and 5 and 10  $\mu$ s central-transition selective <sup>17</sup>O 90° and 180° pulses, respectively. In the case of PDLF a windowed R18,<sup>5</sup> recoupling sequence was used with a 50% window size. The QCPMG spikelet separation was set to 1250 Hz and 6250 Hz for the PRESTO-QCPMG and wPDLF-QCPMG measurements, respectively.

## Acknowledgements

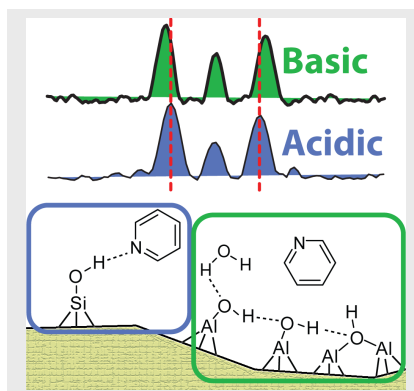
This research was supported by the U.S. Department of Energy, Office of Basic Energy Sciences, Division of Chemical Sciences, Geosciences, and Biosciences through the Ames Laboratory. Partial support for F. P. was through a Spedding Fellowship funded by the Laboratory Directed Research and Development (LDRD) program at the Ames Laboratory. The Ames Laboratory is operated for the U.S. Department of Energy by Iowa State University under Contract No. DE-AC02-07CH11358. F. P. thanks NSERC (National Sciences and Engineering Research Council of Canada) and the Government of Canada for a Banting Postdoctoral Fellowship.

**Keywords:** Brønsted acidity • DNP SENS • heterogeneous catalysis • solid-state NMR spectroscopy • natural-abundance <sup>17</sup>O

- [1] M. Guisnet, P. Magnoux, *Appl. Catal.* **1989**, *54*, 1-27.  
 [2] A. Corma, *Chem. Rev.* **1995**, *95*, 559-614.  
 [3] a) Y. Jiang, J. Huang, W. Dai, M. Hunger, *Solid State Nucl. Magn. Reson.* **2011**, *39*, 116-141; b) M. Valla, A. J. Rossini, M. Caillot, C. Chizallet, P. Raybaud, M. Digne, A. Chaumonnot, A. Lesage, L. Emsley, J. A. van Bokhoven, C. Copéret, *J. Am. Chem. Soc.* **2015**, *137*, 10710-10719; c) A. R. Mouat, C. George, T. Kobayashi, M. Pruski, R. P. van Duyn, T. J. Marks, P. C. Stair, *Angew. Chem. Int. Ed.* **2015**, *54*, 13346-13351; d) Z. Wang, Y. Jiang, O. Lafon, J. Trébosc, K. D. Kim, C. Stampfl, A. Baiker, J.-P. Amoureux, J. Huang, *Nature Comm.* **2016**, in press;  
 [4] M. Hunger, *Catal. Rev. Sci. Eng.* **1997**, *39*, 345-394.  
 [5] J. E. Readman, N. Kin, M. Ziliox, C. P. Grey, *Chem Commun.* **2002**, 2808-2809.  
 [6] a) L. Peng, Y. Liu, N. Kim, J. E. Readman, C. P. Grey, *Nature Mater.* **2005**, *4*, 216-219; b) L. Peng, H. Huo, Y. Liu, C. P. Grey, *J. Am. Chem. Soc.* **2007**, *129*, 335-346; c) H. Huo, L. Peng, C. P. Grey, *J. Chem. Phys. C* **2011**, *115*, 2030-2037.  
 [7] a) F. Blanc, L. Sperrin, D. A. Jefferson, S. Pawsey, M. Rosay, C. P. Grey, *J. Am. Chem. Soc.* **2013**, *135*, 2975-2978; b) F. A. Perras, T. Kobayashi, M. Pruski, *J. Am. Chem. Soc.* **2015**, *137*, 8336-8339; c) F. A. Perras, U. Chaudhary, I. I. Slowing, M. Pruski, *J. Phys. Chem. C* **2016**, *120*, 11535-11544; d) N. J. Brownbill, D. Gajan, A. Lesage, L. Emsley, F. Blanc, *Chem. Commun.* **2017**, *53*, 2563.  
 [8] T. Maly, G. T. Debelouchina, V. S. Bajaj, K.-N. Hu, C.-G. Joo, M. L. Mak-Jurkauskas, J. R. Sirigiri, P. C. A. van der Wel, J. Herzfeld, R. J. Temkin, R. G. Griffin, *J. Chem. Phys.* **2008**, *128*, 052211.  
 [9] a) V. K. Michaelis, E. Markhasin, E. Daviso, J. Herzfeld, R. G. Griffin, *J. Phys. Chem. C* **2012**, *3*, 2030-2034; V. K. Michaelis, B. Corzilius, A. A. Smith, R. G. Griffin, *J. Phys. Chem. B* **2013**, *117*, 14894-14806.  
 [10] a) A. Lesage, M. Lelli, D. Gajan, M. A. Caporini, V. Vitzthum, P. Miéville, J. Alauzun, A. Roussey, C. Thieuleux, A. Mehdi, C. Bodenhausen, C. Copéret, L. Emsley, *J. Am. Chem. Soc.* **2010**, *132*, 15459-15461; b) A. J. Rossini, A. Zagdoun, M. Lelli, A. Lesage, C. Copéret, L. Emsley, *Acc. Chem. Res.* **2013**, *46*, 1942-1951; c) T. Kobayashi, F. A. Perras, I. I. Slowing, A. D. Sadow, M. Pruski, *ACS Catal.* **2015**, *5*, 7055-7062; d) M. A. Hope, D. M. Halat, P. C. M. M. Magusin, S. Paul, L. Peng, C. P. Grey, *Chem. Commun.* **2017**, *53*, 2142-2145.  
 [11] a) A. A. Tsyganenko, P. P. Mardilovich, *J. Chem. Soc., Faraday Trans.* **1996**, *92*, 4843-4852; b) M. Taoufik, K. C. Szeto, N. Merle, I. Del Rosal, L. Maron, J. Trébosc, G. Tricot, R. M. Gauvin, L. Delevoye, *Chem. Eur. J.* **2014**, *20*, 4038-4046.  
 [12] X. Xue, M. Kanzaki, *J. Phys. Chem. B* **2001**, *105*, 3422-3434.  
 [13] T. H. Walter, E. Oldfield, *J. Phys. Chem.* **1989**, *93*, 6744-6751.  
 [14] N. Merle, J. Trébosc, A. Baudouin, I. Del Rosal, L. Maron, K. Szeto, M. Genelot, A. Mortreux, M. Taoufik, L. Delevoye, R. M. Gauvin, *J. Am. Chem. Soc.* **2012**, *134*, 9263-9275.  
 [15] X. Zhao, W. Hoffbauer, J. S. auf der Günne, M. H. Levitt, *Solid State Nucl. Magn. Reson.* **2004**, *26*, 57-64.  
 [16] F. H. Larsen, J. Skibsted, H. J. Jakobsen, N. C. Nielsen, *J. Am. Chem. Soc.* **2000**, *122*, 7080-7086.  
 [17] J. B. Peri, *J. Phys. Chem.* **1965**, *69*, 220-230.  
 [18] A. A. Gurinov, Y. A. Rozhkova, A. Zukal, J. Čejka, I. G. Shenderovich, *Langmuir* **2011**, *27*, 12115-12123.  
 [19] a) S. V. Dvinskikh, H. Zimmermann, A. Maliniak, D. Sandström, *J. Magn. Reson.* **2004**, *168*, 194-201; b) A. Gansmüller, J.-P. Simorre, S. Hediger, *J. Magn. Reson.* **2013**, *234*, 154-164.  
 [20] X. Lu, H. Zhang, M. Lu, A. J. Vega, G. Hou, T. Polenova, *Phys. Chem. Chem. Phys.* **2016**, *18*, 4035-4044  
 [21] M. Edén, *Chem. Phys. Lett.* **2003**, *378*, 55-64.  
 [22] N. C. Nelson, Z. Wang, P. Naik, J. S. Manzano, M. Pruski, and I. I. Slowing, *J. Mat. Chem. A* **2017**, *5*, 4455-4466.  
 [23] a) D. A. Sverjensky, N. Sahai, *Geochim. Cosmochim. Acta* **1996**, *60*, 3773-3797; b) J. A. Schwartz, C. T. Driscoll, and A. K. Bhanot, *J. Colloid Interface Sci.* **1984**, *97*, 55-61; L. A. De Faria, S. Trasatti, *J. Colloid Interface Sci.* **1994**, *167*, 352-357.  
 [24] F. Kontaxis, G. M. Clore, A. Bax, *J. Magn. Reson.* **2000**, *143*, 184-196.  
 [25] a) D. A. Case, *J. Biomol. NMR* **1999**, *15*, 95-102; b) L. Yao, B. Vögeli, J. Ying, A. Bax, *J. Am. Chem. Soc.* **2008**, *130*, 16518-16520.  
 [26] X. Zhao, J. L. Sudmeier, W. W. Bachovchin, M. H. Levitt, *J. Am. Chem. Soc.* **2001**, *123*, 11097-11098.  
 [27] a) J. A. Lercher, H. Noller, *J. Catal.* **1982**, *77*, 152-158; b) D. A. Sverjensky, *Geochim. Cosmochim. Acta* **1994**, *58*, 3123-3129.  
 [28] a) P. Lorente, I. G. Shenderovich, N. S. Golubev, G. S. Denisov, G. Buntkowsky, H.-H. Limbach, *Magn. Reson. Chem.* **2001**, *39*, S18-S29; b) I. G. Shenderovich, G. Buntkowsky, A. Schreiber, E. Gedat, S. Sharif, J. Albrecht, N. S. Golubev, G. H. Findenegg, H.-H. Limbach, *J. Phys. Chem. B* **2003**, *107*, 11924-11939.  
 [29] M.-P. Gaigeot, M. Sprik, M. Sulpizi, *J. Phys.: Condens. Matter* **2012**, *24*, 124106.  
 [30] A. Zagdoun, G. Casano, O. Ouari, M. Schwarzwälder, A. J. Rossini, F. Aussenac, M. Yulikov, G. Jeschke, C. Copéret, A. Lesage, P. Tordo, L. Emsley, *J. Am. Chem. Soc.* **2013**, *135*, 12790-12797.

## COMMUNICATION

**The lonely reporter:** DNP SENS is applied to enable natural-abundance  $^{17}\text{O}$ - $^1\text{H}$  distance measurements in silica and silica-alumina materials. This highly-precise (sub-pm) measurement of O-H bond lengths can be used to probe the Brønsted acidity of oxide surfaces as well as detect the formation of intermolecular hydrogen bonding interactions.



Frédéric A. Perras, Zhuoran Wang,  
Pranjali Naik, Igor I. Slowing, and Marek  
Pruski\*

Page No. – Page No.

**Natural Abundance  $^{17}\text{O}$  DNP SENS  
Provides  $^{17}\text{O}$ - $^1\text{H}$  Distances with Sub-  
Picometer Precision and Insights into  
Brønsted Acidity**